Preprints of the 18th IFAC World Congress
Milano (Italy) August 28 - September 2, 2011

Switching Model Predictive Control for a Quadrotor Helicopter under Severe Environmental Flight Conditions

K. Alexis [1], **G. Nikolakopoulos**, **Y. Koveos** and **A. Tzes**

Electrical and Computer Engineering Department,
University of Patras,
Rio 26500, Greece.

Abstract: In this article a switching Model Predictive Controller for the attitude and hovering control of a prototype Unmanned quadrotor Helicopter (UqH) subject to atmospheric disturbances is presented. The control scheme is computed based on Piecewise Affine (PWA) models of the UqH's attitude and altitude dynamics, where the effects of the atmospheric turbulence are taken into consideration as additive disturbances. The switching of the MPC scheme is ruled by the estimation and the rate of the rotation angles, for the altitude and attitude control correspondingly. Extended experimental studies indicate the overall scheme's efficiency in hovering scenarios despite the applied wind–disturbances.

Keywords: Unmanned Aerial Vehicles, Disturbance Attenuation, Model Predictive Control.

1. INTRODUCTION

Recently, the area of Unmanned Aerial Vehicles (UAVs) has seen rapid growth, mainly due to the ability of UAVs to effectively carry out a wide range of applications with low cost and without putting human resources at risk. The aforementioned extended set of possible applications imposes new demands in the area of control and navigation in order to design Unmanned Systems capable of operating inside harsh environments and coping with complex missions. Moreover, as the UAV–involving applications become more complex the need for air vehicles, with enough processing power and modular connectivity with a wide set of sensors, rises.

In this article, a novel prototype Unmanned quadrotor Helicopter, depicted in Figure 1, is being utilized as the experimental set–up for the application of the proposed novel MPC scheme. Until now in the relevant literature of Unmanned quadrotor Helicopters, the problem of control design has been addressed by a large number of publications that primarily focus in the following areas: a) the development of PID controllers and LQ–Regulators [Bouabdallah et al. (2004); Hoffmann et al. (2007)], b) Nonlinear control methods including Sliding Mode controllers [Benallegue et al. (2006)], Backstepping control approaches in [Bouabdallah and Siegwart (2007)], an Integral predictive–nonlinear H_∞ control [Raffo et al. (2010)], and c) a Constrained Finite Time Optimal Control Scheme [Alexis et al. (2010)]. In addition, in most of the existing literature of rotorcrafts, research efforts on the effects of the environmental disturbances [Yang et al. (2009)] have focused primarily in simulation studies; while an experimental verification is still needed to validate the efficiency of the noted efforts. This article extends the results of the attitude control for a quadrotor [Alexis et al. (2010)] to the altitude control, based on a PWA modeling and switching MPC approach. More specifically the main control novelties include: a) the Piecewise Affine modeling of the attitude and altitude dynamics of the UqH providing the capability to develop control actions for a larger part of the helicopter flight envelope, b) the modeling of the perturbations induced by wind–gusts as output disturbances, and c) the development of a switching Model Predictive Controller that accounts for the physical and mechanical constraints of the quadrotor. The linearization of the UqH's attitude and altitude dynamics at several operating points, combined with the additive disturbance terms, result in a family of PWA linear systems, where each one is valid for a subset of the flight envelope of the helicopter. The resulting MPC scheme provides the optimal control for each region of the flight envelope while ensuring the smooth transition of the control effort, as the UqH switches from one region to its neighboring ones.

Fig. 1. UPATcopter prototype Unmanned quadrotor Helicopter

This article is structured as follows. In Section 2, the modeling approach for the attitude and altitude dynamics of a UqH is presented followed by the mathematical formulation of the physical constraints and the effects of wind disturbances. In Section 3, the design and the development of the switching MPC scheme is analyzed for the quadrotor's attitude tracking control problem and stable hovering. In Section 4, the prototype quadrotor is presented followed by the presentation of extended experimental results that prove the efficacy of the proposed control scheme. Conclusions are drawn in Section 5.

[1] Corresponding Author's e-mail kostalexis@ece.upatras.gr

2. QUADROTOR HELICOPTER DYNAMICS

The modeling procedure, assumes that the structure is rigid and symmetrical, the center of gravity and the body fixed frame origin coincide, the propellers are rigid and the thrust and drag forces are proportional to the square of propeller's speed. Two coordinate systemsare utilized, i.e. a) the Body–fixed frame $\mathbf{B} = [\mathbf{B}_1, \mathbf{B}_2, \mathbf{B}_3]^T$ and b) the Earth–fixed frame $\mathbf{E} = [\mathbf{E}_x, \mathbf{E}_y, \mathbf{E}_z]^T$ as shown in Figure 2.

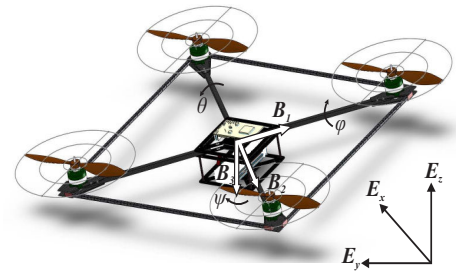

Fig. 2. Quadrotor helicopter configuration frame system

The aerodynamic forces and moments acting on the UqH during a hovering flight segment correspond to the thrust ($\mathbf{T}$), hub forces ($\mathbf{H}$) and drag moment ($\mathbf{Q}$) due to vertical, horizontal and aerodynamic forces respectively, followed by the rolling moment ($\mathbf{R}$) related to the integration over the entire rotor of the lift of each section, acting at a given radius. An extended formulation of these forces and moments can be found at [Bouabdallah and Siegwart (2007)], whereas an in depth analysis on the role of the accelerometers feedback and the propeller aerodynamics can be found at [Martin and Salaun (2010); P. Bristeau and Petit (2009)]. Using the Euler-Lagrange formulation the system can be described by the following set of twelve order nonlinear ODEs of the form:

$$\dot{\mathbf{X}} = f(\mathbf{X}, \mathbf{U}) + \tilde{\mathbf{W}} \tag{1}$$

with $\mathbf{U} \in \Re^5$ the input vector, and $\mathbf{X} \in \Re^{12}$ the state vector that consists of the translational components $\xi = [x,\ y,\ z]^T$ and the rotational components of the UqH with respect to the ground, defined by the vector $\eta = [\phi,\ \theta,\ \psi]^T$. The disturbance vector $\tilde{\mathbf{W}} \in \Re^{12}$ is defined as $\tilde{\mathbf{W}} = [\tilde{\mathbf{W}}_\eta\ ,\ \tilde{\mathbf{W}}_\xi]^T = [0, \tilde{W}_1, 0, \tilde{W}_2, 0, \tilde{W}_3, 0, \tilde{W}_4, 0, \tilde{W}_5, 0, \tilde{W}_6]$. Equation (1) in its augmented form can be stated as:

$$\dot{\mathbf{X}} = \begin{bmatrix} \dot{\phi} \\ \ddot{\phi} \\ \dot{\theta} \\ \ddot{\theta} \\ \dot{\psi} \\ \ddot{\psi} \\ \hline \dot{z} \\ \ddot{z} \\ \dot{x} \\ \ddot{x} \\ \dot{y} \\ \ddot{y} \end{bmatrix} = \begin{bmatrix} \dot{\phi} \\ \dot{\theta}\dot{\psi}a_1 + \dot{\theta}a_2\Omega_r + b_1U_2 \\ \dot{\theta} \\ \dot{\phi}\dot{\psi}a_3 - \dot{\phi}a_4\Omega_r + b_2U_3 \\ \dot{\psi} \\ \dot{\theta}\dot{\phi}a_5 + b_3U_4 \\ \hline \dot{z} \\ g - (\cos\phi\cos\theta)U_1/m \\ \dot{x} \\ (\cos\phi\sin\theta\cos\psi + \sin\varphi\sin\psi)U_1/m \\ \dot{y} \\ (\cos\phi\sin\theta\sin\psi - \sin\varphi\cos\psi)U_1/m \end{bmatrix} + \begin{bmatrix} \tilde{W}_\eta \\ \hline \tilde{W}_\xi \end{bmatrix} \tag{2}$$

$$\mathbf{U} = \begin{bmatrix} U_1 \\ U_2 \\ U_3 \\ U_4 \\ \Omega_r \end{bmatrix} = \begin{bmatrix} b(\Omega_1^2 + \Omega_2^2 + \Omega_3^2 + \Omega_4^2) \\ b(-\Omega_2^2 + \Omega_4^2) \\ b(\Omega_1^2 - \Omega_3^2) \\ d(-\Omega_1^2 + \Omega_2^2 - \Omega_3^2 + \Omega_4^2) \\ -\Omega_1 + \Omega_2 - \Omega_3 + \Omega_4 \end{bmatrix} \tag{3}$$

$$\begin{array}{lll} a_1 = (I_{yy} - I_{zz})/I_{xx} & a_2 = J_r/I_{xx} & a_3 = (I_{zz} - I_{xx})/I_{yy} \\ a_4 = J_r/I_{yy} & a_5 = (I_{xx} - I_{yy})/I_{zz} & b_1 = l_a/I_{xx} \\ b_2 = l_a/I_{yy} & b_3 = 1/I_{zz} & \end{array} \tag{4}$$

The input $U_1 \in \Re$ is related to the total thrust, the inputs $U_2, U_3, U_4 \in \Re$ are related to the rotations of the quadrotor, and $\Omega_r \in \Re$ is the overall residual propeller angular speed. The rest of the utilized parameters in equation (2) are listed in Table 1.

Table 1. UqH model Parameters

I_{xx}	Moment of Inertia of the UqH about the X axis
I_{yy}	Moment of Inertia of the UqH about the Y axis
I_{zz}	Moment of Inertia of the UqH about the Z axis
l_a	UqH Arm length
b	Thrust coefficient
d	Drag coefficient
J_m	Moment of inertia of the motor about its axis of rotation
J_p	Moment of inertia of the propeller about its axis of rotation
$J_r = J_m + J_p/4$	Moment of inertia of the rotor about its axis of rotation

Since the angles η and their derivatives $\dot{\eta}$ are independent of the translational–vector component $(\xi, \dot{\xi})$ the aforementioned system's attitude dynamics in equation (2) can be decoupled from the translational ones [Bouabdallah and Siegwart (2007)]. Since, this article focus on the hovering control, and as a result in the quadrotor's model described in equations (5) and (6), only the attitude and altitude dynamics have been taken under consideration in the modeling procedure, while the other two translational states (x, y) are left uncontrolled. Under this consideration two hierarchically connected subsystems are derived, namely the vertical motion and the rotational motions subsystems.

$$\text{Altitude Dynamics: } \begin{bmatrix} \dot{z} \\ \ddot{z} \end{bmatrix} = \begin{bmatrix} \dot{z} \\ g - (\cos\phi\cos\theta)U_1/m \end{bmatrix} + \begin{bmatrix} 0 \\ \tilde{W}_4 \end{bmatrix} \tag{5}$$

$$\text{Attitude Dynamics: } \begin{bmatrix} \dot{\phi} \\ \ddot{\phi} \\ \dot{\theta} \\ \ddot{\theta} \\ \dot{\psi} \\ \ddot{\psi} \end{bmatrix} = \begin{bmatrix} \dot{\phi} \\ \dot{\theta}\dot{\psi}a_1 + \dot{\theta}a_2\Omega_r + b_1U_2 \\ \dot{\theta} \\ \dot{\phi}\dot{\psi}a_3 - \dot{\phi}a_4\Omega_r + b_2U_3 \\ \dot{\psi} \\ \dot{\theta}\dot{\phi}a_5 + b_3U_4 \end{bmatrix} + \tilde{W}_\eta \tag{6}$$

3. MODEL PREDICTIVE CONTROL SCHEME

The design of the proposed MPC–scheme is based on two decoupled switching MP–controllers applied on the multiple PWA representations of the rotational subsystem [Alexis et al. (2010)] and on the error dynamics modeling for the quadrotor's altitude [Raffo et al. (2010)]. The overall block diagram of the closed loop system is depicted in Figure 3.

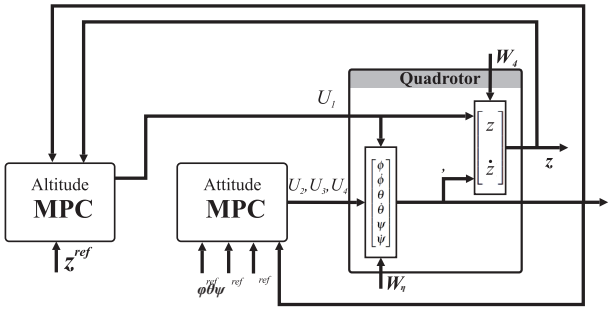

Fig. 3. Hovering Model Predictive Control Scheme

By transforming the altitude dynamics in equation (5) into error dynamics and discretizing with a T_s sampling time the following PWA state space representation ($\mathbf{x}^z = [\tilde{z}(t), \tilde{w}(t), \int \tilde{z}(t)dt]^T =$

$[z-z^r, w-w^r, \int z-z^r dt]^T, w=\dot{z})$, can be extracted [Raffo et al. (2010)]:

$$\mathbf{x}^z(k+1) = \begin{bmatrix} \tilde{z}(t) \\ \tilde{w}(t) \\ \int \tilde{z}(t)dt \end{bmatrix} = \bar{\mathbf{A}}_z \mathbf{x}^z(k) + \bar{\mathbf{B}}_j^z u^z(k) + \tilde{\mathbf{w}}^z, k \in Z^+ \quad (7)$$

$$\bar{\mathbf{A}}^z = \begin{bmatrix} 1 & T_s & 0 \\ 0 & 1 & 0 \\ T_s & 0 & 1 \end{bmatrix}, \ \bar{\mathbf{B}}_j^z = \begin{bmatrix} 0 \\ \frac{T_s}{m}\cos\theta(k)\cos\phi(k) \\ 0 \end{bmatrix}$$

$$u_z = [\delta U_1]$$

where in $\bar{B}_j^z$ the index $j \in \mathscr{Z}^+$ indicates the various linearizarization matrices that can be extracted based on estimation of the θ and ϕ rotation angles. Similarly as it has been presented in [Alexis et al. (2010)] the attitude dynamics in equation (6), can also be modeled as a set of PWA systems, linearized for different attitude operation points $\mathbf{x}_\eta^{\circ,\mathbf{j}} = \left[0, \dot{\phi}^{\circ,j}, 0, \dot{\theta}^{\circ,j}, 0, \dot{\psi}^{\circ,j}\right]^T$, described by the following set of discrete time state space equations:

$$\mathbf{x}^\eta(k+1) = \mathbf{A}_\mathbf{j}^\eta \mathbf{x}^\eta(k) + \mathbf{B}_\mathbf{j}^\eta \mathbf{u}^\eta(k) + \tilde{\mathbf{w}}^\eta \quad (8)$$

$$\mathbf{u}^\eta = [\delta U_1, \delta U_2, \delta U_3, \delta U_4, \delta\Omega_r]^T$$

where,

$$\mathbf{A_j}^\eta = \begin{bmatrix} 0 & 1 & 0 & 0 & 0 & 0 \\ 0 & 0 & 0 & \frac{I_{yy}-I_{zz}}{I_{xx}}\dot{\psi}^{\circ,j} & 0 & \frac{I_{yy}-I_{zz}}{I_{xx}}\dot{\theta}^{\circ,j} \\ 0 & 0 & 0 & 1 & 0 & 0 \\ 0 & \frac{I_{zz}-I_{xx}}{I_{yy}}\dot{\psi}^{\circ,j} & 0 & 0 & 0 & \frac{I_{zz}-I_{xx}}{I_{yy}}\dot{\phi}^{\circ,j} \\ 0 & 0 & 0 & 0 & 0 & 1 \\ 0 & \frac{I_{xx}-I_{yy}}{I_{zz}}\dot{\theta}^{\circ,j} & 0 & \frac{I_{xx}-I_{yy}}{I_{zz}}\dot{\phi}^{\circ,j} & 0 & 0 \end{bmatrix} \quad (9)$$

$$\mathbf{B_j}^\eta = \begin{bmatrix} 0 & 0 & 0 & 0 & 0 \\ 0 & \frac{l_a}{I_{xx}} & 0 & 0 & \frac{J_r}{I_{xx}}\dot{\theta}^{\circ,j} \\ 0 & 0 & 0 & 0 & 0 \\ 0 & 0 & \frac{l_a}{I_{yy}} & 0 & \frac{J_r}{I_{yy}}\dot{\theta}^{\circ,j} \\ 0 & 0 & 0 & 0 & 0 \\ 0 & 0 & 0 & \frac{1}{I_{zz}} & 0 \end{bmatrix} \quad (10)$$

and $\mathbf{u}^\eta$ is the vector that contains the small alterations on the control movements.

The adopted PWA modeling is utilized for the controller design procedure, letting the MPC–scheme to count for a larger set of the UqH's flight envelope and produce more precise control actions as more linearization points are taken under consideration.

3.1 MPC Synthesis

The construction of the MP–Controllers for each vertical and rotary motion ($[z\ \dot{z}]^T, [\eta\ \dot{\eta}]^T$) subsystem follows the same uniform methodology. By considering a $T_s \in \Re^+$ sampling period, all equations (7,8) in the discrete time space can be cast as a PWA system:

$$\mathbf{x}_{k+1}^\ell = \mathbf{A}_\mathbf{j}^{*,\ell}\mathbf{x}_k^\ell + \mathbf{B}_\mathbf{j}^{*,\ell}\mathbf{u}_k^\ell + \tilde{\mathbf{w}}^\ell \ ; \quad k \in Z^+ \quad (11)$$

where $\mathbf{x}_k^\ell \in \mathscr{X}^\ell$, $\ell \to [z, \eta]$ is the discrete state vector of each system, $\mathbf{u}_k^\ell \in \mathscr{U}^\ell$ is the corresponding control action at the discrete time instant k, and $\mathbf{A}_\mathbf{j}^{*,\ell}$, $\mathbf{B}_\mathbf{j}^{*,\ell}$ are the discrete time versions of the state space matrices. Moreover, $j \in \mathscr{S}$ with $\mathscr{S} \triangleq \{1, 2, \cdots, s\}$ a finite set of indexes and s denotes the number of piecewise affine sub–systems in (11). For polytopic uncertainty, Σ is the polytope $\mathrm{Co}\{[\mathbf{A_1}^{*,\ell}\ \mathbf{B_1}^{*,\ell}], \cdots, [\mathbf{A_s}^{*,\ell}\ \mathbf{B_s}^{*,\ell}]\}$, Co denotes the convex hull and $[\mathbf{A_i}^{*,\ell}, \mathbf{B_i}^{*,\ell}]$ are vertices of the convex hull. Any $[\mathbf{A}^{*,\ell}\ \mathbf{B}^{*,\ell}]$ within the convex set Σ is a linear combination of the vertices $[\mathbf{A}^{*,\ell}\ \mathbf{B}^{*,\ell}] = \sum_{j=1}^L a_j [\mathbf{A_i}^{*,\ell}\ \mathbf{B_i}^{*,\ell}]$ with $\sum_{j=1}^L a_j = 1,\ 0 \le a_j \le 1$.

The sets $\mathscr{X}^\ell$ and $\mathscr{U}^\ell$ specify state and input constraints and it is assumed they are compact polyhedral sets that contain the origin in their interior. For simplicity we assume that the origin is an equilibrium state $\mathbf{x}_k^{\ell,o,j}$, with $\mathbf{u}^\ell(0) = \mathbf{0}$. For the j–th linearized subsystem, let the set $\mathscr{X}_i^\ell$ contain the $\mathbf{x}_i^{\ell,o}$ states that satisfy the following bounding inequality:

$$\mathbf{x}_i^{\ell,\circ,j} \in \mathscr{X}^\ell \ : \ \mathbf{x}_i^{\ell,\circ,j,\min} = \mathbf{x}_i^{\ell,\circ,j} - \Delta_i^\ell \le \mathbf{x}^{\ell,\circ,j} \le \mathbf{x}^{\ell,\circ,j} + \Delta_i^\ell = \mathbf{x}_i^{\ell,\circ,j,\max} \quad (12)$$

where the subscript index corresponds to the i–th component of the x–vector (i.e. $i=2, \ell \to \eta$ corresponds to the $\dot{\phi}^{\circ,j}$–variable), $\Delta_i^\ell \in \Re^+$ and $\mathscr{X} = \bigcup \mathscr{X}_i^\ell$, $i = 1, \cdots, m$, where m denotes the length of $x^{\ell,\circ,j}$. For the MPC–synthesis test–cases the following state constraints have been utilized, while the rest of the states are unconstrained.

$$\begin{bmatrix} -\frac{\pi}{2} \\ -\pi \\ -0.75 \\ -1 \\ -1 \end{bmatrix} < \begin{bmatrix} \phi, \theta \\ \psi \\ \dot{\phi}, \dot{\theta} \\ \dot{\psi} \\ \tilde{w} \end{bmatrix} < \begin{bmatrix} \frac{\pi}{2} \\ \pi \\ 0.75 \\ 1 \\ 1 \end{bmatrix} \quad (13)$$

.

The control inputs bounding set $\mathscr{U}$ can be derived by the bounds on the motors' angular velocities Ω_i, $i = 1, ..., 4$, , $\Omega_i \in [0, \Omega_i^{\max}]$ and by utilizing interval analysis. As a result the constraints on the control inputs are formulated as shown in (14).

$$\begin{aligned} \delta U_1^{\min} &= 0 \le \delta U_1 \le b\sum_{i=1}^4 (\Omega_1^{\max})^2 = \delta U_1^{\max} \\ \delta U_2^{\min} &= -b(\Omega_2^{\max})^2 \le \delta U_2 \le b(\Omega_4^{\max})^2 = \delta U_2^{\max} \\ \delta\delta U_3^{\min} &= -b(\Omega_3^{\max})^2 \le \delta U_3 \le b(\Omega_1^{\max})^2 = \delta U_3^{\max} \\ \delta U_4^{\min} &= -d[(\Omega_1^{\max})^2 + (\Omega_3^{\max})^2] \le \delta U_4 \le d[(\Omega_2^{\max})^2 + (\Omega_4^{\max})^2] = \delta U_4^{\max} \\ \delta\Omega_r{}^{\min} &= -\Omega_1^{\max} - \Omega_3^{\max} \le \delta\Omega_r \le \Omega_2^{\max} + \Omega_4^{\max} = \delta\Omega_r{}^{\max} \end{aligned} \quad (14)$$

and $\mathscr{U} = \bigcup \mathscr{U}_i$, $i = 1, \cdots, 7$. The state and input constraints are formulated using a set of $\mathbf{H_i}^l$ zeroed $2 \times (m+l)$ matrices except for their i–th column which is equal to $[1, -1]^T$, where m is the number of states of vector x^l and n the number of control actions u^l. Specifically, for each of the individual subsystems on the basis of which the controller is constructed, the constraints are formulated as follows.

Vertical motion subsystem:

$$\begin{bmatrix}\mathbf{H}_1^z\\ \mathbf{H}_2^z\\ \mathbf{H}_3^z\\ \mathbf{H}_4^z\end{bmatrix}_{8\times 4}\cdot\begin{bmatrix}\mathbf{x}^z\\ --\\ \mathbf{u}^z\end{bmatrix}_{4\times 1}\leq\begin{bmatrix}x_1^{z,\circ,j,\max}+\varepsilon V_{j\ \max}^x\\ x_1^{z,\circ,j,\min}-\varepsilon V_{j\ \max}^x\\ x_2^{z,\circ,j,\max}+\varepsilon V_{j\ \max}^x\\ x_2^{z,\circ,j,\min}-\varepsilon V_{j\ \max}^x\\ x_3^{z,\circ,j,\max}+\varepsilon V_{j\ \max}^x\\ x_3^{z,\circ,j,\min}-\varepsilon V_{j\ \max}^x\\ --\\ \delta U_1^{\max}\\ \delta U_1^{\min}\end{bmatrix}\tag{15}$$

Attitude subsystem:

$$\begin{bmatrix}\mathbf{H}_1^\eta\\ \vdots\\ \mathbf{H}_6^\eta\\ --\\ \mathbf{H}_7^\eta\\ \vdots\\ \mathbf{H}_{11}^\eta\end{bmatrix}_{22\times 11}\cdot\begin{bmatrix}\mathbf{x}^\eta\\ --\\ \mathbf{u}^\eta\end{bmatrix}_{11\times 1}\leq\begin{bmatrix}x_1^{\circ,j,\max}+\varepsilon V_{j\ \max}^x\\ \vdots\\ x_1^{\circ,j,\min}-\varepsilon V_{j\ \max}^x\\ x_6^{\circ,j,\max}+\varepsilon V_{j\ \max}^x\\ x_6^{\circ,j,\min}-\varepsilon V_{j\ \max}^x\\ --\\ \delta U_1^{\max}\\ \delta U_1^{\min}\\ \vdots\\ \delta\\ \delta\Omega_r^{\max}\\ \delta\Omega_r^{\min}\end{bmatrix}\tag{16}$$

,

where $V_{j\ \max}^x$ are the relaxation vectors that have nonnegative entries and are being utilized for relaxing the corresponding constraints and $\varepsilon\in\Re^+$ a small constant number. These constraints are embedded in the Model Predictive Control computation algorithm in order to compute an optimal controller that counts for the physical and mechanical constraints that restrict the UqH motion.

The $\tilde{\mathbf{w}}^\ell$ term corresponds to the effect of the unknown additive disturbance (such as a wind gust) on the system's dynamics and can be analyzed as $\tilde{\mathbf{w}}^\ell=\mathbf{B}_d^\ell\mathbf{d}^\ell(\mathbf{k})$. The disturbance effects are modeled as the output of the following linear time invariant system:

$$\begin{aligned}\mathbf{x}_d^\ell(k+1)&=\hat{\mathbf{A}}_\ell\mathbf{x}_d^\ell(k)+\hat{\mathbf{B}}_\ell\mathbf{n}_d^\ell(k)\\ \mathbf{d}^\ell(k)&=\hat{\mathbf{C}}_\ell\mathbf{x}_d^\ell(k)+\hat{\mathbf{D}}_\ell\mathbf{n}_d^\ell(k)\end{aligned}\tag{17}$$

. The system described in (17) is driven by random Gaussian noise $\mathbf{n}_d^\ell(k)$, having zero mean and unit covariance matrix. For white noise unmeasured disturbances, it is modeled as the output of an integrator. The bounds for the disturbance $\mathbf{d}^\ell$ are assumed to be known and in the work presented in this article, those bounds were experimentally measured by applying forcible gusts and measuring the maximum effect of them in the UqH's attitude.

In a generic framework, the (ℓ,j)–th switching MP–controller's objective is to optimize the quadratic cost in (18), while the (ℓ,j)–th–discrete linearized system is within Σ^ℓ. The model predictive controller $V_{MPC}^{\ell,j}(k)$ corresponding to the ℓ,j-th PWA model of the UqH's motion at time k is obtained by solving the following optimization problem with respect to the small control moves Δu^ℓ and to the relaxing slack variable ε, with $\varepsilon\geq 0$:

$$\begin{aligned}\underset{\Delta u(k|k)^l,\cdots,\Delta u(m-1+k|k)^l}{J(\Delta u^\ell,\varepsilon)}=&\sum_{i=0}^{p-1}[\mathbf{y}^\ell(k+i+1|k)-\mathbf{r}^\ell(k+i+1)]^T\mathbf{Q}^\ell[\mathbf{y}^\ell(k+i+1|k)\\ &-\mathbf{r}^\ell(k+i+1)]+\Delta\mathbf{u}^\ell(k+i|k)^T\mathbf{R}^\ell_{\Delta\mathbf{u}^\ell}\Delta\mathbf{u}^\ell(k+i|k)+\\ &[\mathbf{u}^\ell(k+i|k)-\mathbf{u}^\ell{}_{target}(k+i)]^T\mathbf{R}^\ell_{\mathbf{u}^\ell}[\mathbf{u}^\ell(k+i|k)\\ &-\mathbf{u}^\ell{}_{target}(k+i)]+\rho_e\varepsilon^2\end{aligned}\tag{18}$$

where p, m are the prediction and control horizon respecively, $\mathbf{Q}^\ell$ and $\mathbf{R}_{\Delta\mathbf{u}^\ell}$ and $\mathbf{R}^\ell_{\mathbf{u}}$ are the penalty matrices, all positive semi-definite. Moreover, $\mathbf{y}^\ell$, $\mathbf{r}^\ell$ are the output and the reference signals of the controlled system, while no bounds have been considered for the control moves $\Delta\mathbf{u}^\ell$. The weight ρ_e on the slack variable ε penalizes the violation of the constraints, while $\mathbf{u}^\ell_{target}(k+i)$ is a setpoint for the input vector. The subscript $()_j$ denotes the $j-th$ component of a vector, while $k+i|k$ denotes the predicted value for time $k+i$ based on the information available a the k–time instant; $\mathbf{r}^\ell(k)$ is the current sample of the output reference, subject to the constraints in (15-16), with respect to the sequence of input increments $\{\Delta\mathbf{u}(k|k),\cdots,\Delta\mathbf{u}^\ell(m-1+k|k\}$ and to the slack variable ε, and by setting $\mathbf{u}^\ell(k)=\mathbf{u}^\ell(k-1)+\Delta\mathbf{u}^\ell(k|k)^*$, where $\Delta\mathbf{u}^\ell(k|k)^*$ is the first element of the resulting optimal sequence. Once all $V_{MPC}^{\ell,j}(k)$ controllers are computed, the total controller is produced in a connected between the sub–controllers and switching inside them manner, with the switching function governed by the state vectors $\mathbf{x}^\ell$.

Under the assumption of (ℓ,s) discrete linear systems and (ℓ,s) available $V_{MPC}^{\ell,j}$ controllers, the objective of the $j\in\mathscr{S}^\ell$ controller is to stabilize the (ℓ,j)–th system. If s increases, then the approximation of the nonlinear system by a large number of linearized systems is more accurate and results in greater envelops of flights, and this allows the integration of the solution to the system's non–linear dynamics in (1) as a close match to the solution of the system's time varying linearized dynamics. As the vector $\mathbf{x}_d^\ell(k)$ is not directly measurable, predictions are obtained based on an extended Kalman state estimator, based on (11) and (17):

$$\begin{bmatrix}\mathbf{x}^\ell(k+1)\\ \mathbf{x_d}^\ell(k+1)\end{bmatrix}=\begin{bmatrix}\mathbf{A}_j^{*,\ell} & \mathbf{B_d}^\ell\hat{\mathbf{C}}^\ell\\ 0 & \hat{\mathbf{A}}^\ell\end{bmatrix}\begin{bmatrix}\mathbf{x}^\ell(k)\\ \mathbf{x_d}^\ell(k)\end{bmatrix}+\begin{bmatrix}\mathbf{B}_j^{*,\ell}\\ 0\end{bmatrix}\mathbf{u}^\ell(k)+\begin{bmatrix}\mathbf{B_d}^\ell\hat{\mathbf{D}}^\ell\\ \hat{\mathbf{B}}^\ell\end{bmatrix}\mathbf{n_d}^\ell(k)\tag{19}$$

.

4. EXPERIMENTAL STUDIES

The main novelty of the quadrotor prototype design presented is the utilization of an advanced processing Main Control Unit (MCU) Kontron pITX Single Board Computer (SBC) equipped with an ATOM Z530 1.6GHz CPU with 2GB of RAM running Microsoft Windows XP OS, installed in a Solid State D Hard Disk Drive. The SBC is the core of the UqH. An XSens Mti-G Attitude and Heading Reference System is utilized to provide attitude estimations, where an AVR microcontroller is utilized to communicate with the brushless Electronic Speed Controllers (ESCs) via I2C protocol while concurrently providing Sonar–based altitude data to the SBC. The main control loop is programmed relying on NI's LabVIEW environment at the SBC while safety functions are implemented in the AVR microcontroller. Sonar–based altitude data are transmitted to the AVR microcontroller through I2C bus and afterwards these data are forwarded to the SBC. Note that a posteriori altitude sonar data are combined with $\ddot{z}$ measurements and $\dot{z}$ estimations using Extended Kalman Filter algorithm [Simon (2006)]. This provides the capability to have estimations of the altitude states, a fact that makes possible the efficient control of the system. The UqH prototype is equipped with a Wi-Fi 802.11n adaptor which is both utilized for telemetry and communication with other systems. The main design variables are listed in Table 2. The inertia of the system has been calculated using the 3D model of the system and CFD techniques. Based on the listed values the following constraints on the inputs can be set as $0\leq U_1\leq 19.775$, $|U_2|\leq 9.818$, $|U_3|\leq 9.818$, $|U_4|\leq 0.22$.

Table 2. UqH model Parameters

Design Variable	Value	Units
m	1.1	kg
l_a	0.21	m
I_{xx}	0.32	$kg \cdot m^2$
I_{yy}	0.32	$kg \cdot m^2$
I_{zz}	0.49	$kg \cdot m^2$
J_r	$6.5 \cdot 10^{-4}$	$kg \cdot m^2$
b	$4.9 \cdot 10^{-5}$	$N \cdot sec^2$
d	$11 \cdot 10^{-7}$	$N - m \cdot sec^2$

The tuning parameters of the switching MPC were $\mathbf{R}^{\eta}_{\mathbf{u}^{\eta}_{\mathbf{j}},j} = 20 \cdot \mathbf{I}_5$, $\mathbf{R}^{\eta}{}_{\Delta\mathbf{u}^{\eta}_{\mathbf{j}},j} = 200 \cdot \mathbf{I}_5$, and $\mathbf{Q}^{\eta} = 20^4 \cdot \mathbf{I}_6$ for all j attitude PWA utilized subsystems and $\mathbf{R}^{z}_{\mathbf{u}^{\mathbf{z}}_{\mathbf{j}},j} = 10$, $\mathbf{R}^{\mathbf{z}}{}_{\Delta\mathbf{u}^{\mathbf{z}}_{\mathbf{j}},j} = 100$, and $\mathbf{Q}^{\mathbf{z}} = 10^4 \cdot \mathbf{I}_3$ for all j altitude PWA utilized subsystems, the prediction and control horizons were set to $p = 5$ and $m = 2$ respectively, while the robust behavior to disturbances has been calculated for the disturbance vectors $\mathbf{w}^{z}, \mathbf{w}^{\eta}$. The bounds for the additive disturbances, under the wind conditions, have been experimentally measured as: $\mathbf{d}^{\eta} = |\mathbf{w}^{\eta,\max}| = [0, 0.15 \text{ rad/s}, 0, 0.15 \text{ rad/}s, 0, 0.15 \text{ rad/s}]^T$, $\mathbf{d}^{z} = |\mathbf{w}^{\mathbf{z},\max}| = [0, 0.1 \text{ m/s}]^T$.

Table 3. PWA Operation Points

1	-0.01	$<$	$\dot{\phi}^{\circ,j}, \dot{\theta}^{\circ,j}$	$<$	0.01
2	0.01	$<$	$\dot{\phi}^{\circ,j}$	$<$	0.09
3	-0.09	$<$	$\dot{\phi}^{\circ,j}$	$<$	-0.01
4	0.01	$<$	$\dot{\theta}^{\circ,j}$	$<$	0.09
5	-0.09	$<$	$\dot{\theta}^{\circ,j}$	$<$	0.09
6	0.01	$<$	$\dot{\phi}^{\circ,j}$ and $\dot{\theta}^{\circ,j}$	$<$	0.09
7	-0.09	$<$	$\dot{\phi}^{\circ,j}$ and $\dot{\theta}^{\circ,j}$	$<$	-0.01
1	-0.1	$<$	θ, ϕ	$<$	0.3
2			$\lvert\phi\rvert$ or $\lvert\theta\rvert$	$>$	0.3

For the experimental validation of the switch MPC scheme, $s = 9$ attitude PWA–systems were used and $s = 2$ altitude PWA–systems. In all these cases, the sampling period was set to $T_s = 0.01$s. The $\mathbf{A}^{*,\ell}_{j}, \mathbf{B}^{*,\ell}_{j}$ matrices of the PWA systems utilized for the controller computation were computed for regions shown in Table 3.

The efficacy of the proposed control scheme both in attitude and altitude control has been verified in multiple experimental test–cases. The main objective was to confirm the ability of the control law to stabilize the prototype quadrotor under the presence of forcible wind–gusts. The wind–gusts were generated by an electric turbine and the induced gust velocities were measured using a rotary vane anemometer. For all experimental results presented the datalogging frequency was 10Hz while the controller was being updated at 100Hz. For the case of attitude regulation and for an overall thrust that slightly cancels the gravity force, the proposed switching MPC effectively stabilizes the system as presented in Figure 4.

By the integration of the altitude and attitude control stable and precise hover control can be achieved as presented in Figure 5. The ability, of the proposed control strategy to attenuate external disturbances (wind gusts), in the case of the attitude problem, is presented in Figure 6. Moreover, the efficacy of the proposed control scheme, for the case of the hovering problem, is depicted in Figure 7, under the presence of continues forcible wind–gust (Three in the Beaufort scale). This result is very important, as due to the small size of the quadrotor, the aggressive

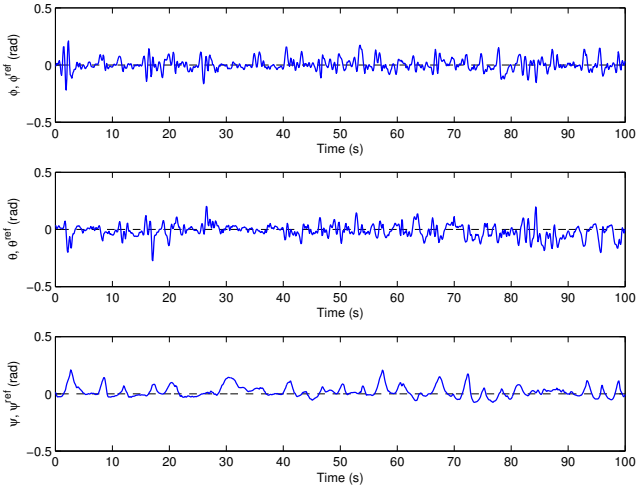

Fig. 4. Attitude regulation in the absence of wind gusts

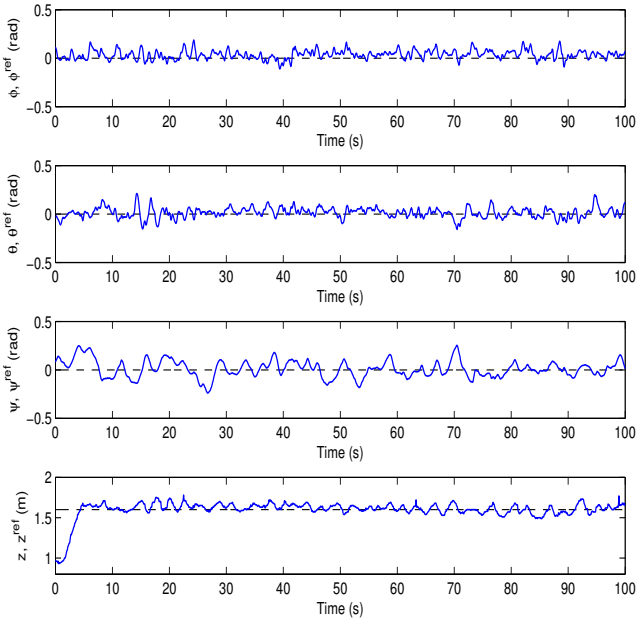

Fig. 5. Stable hovering in the absence of wind gusts

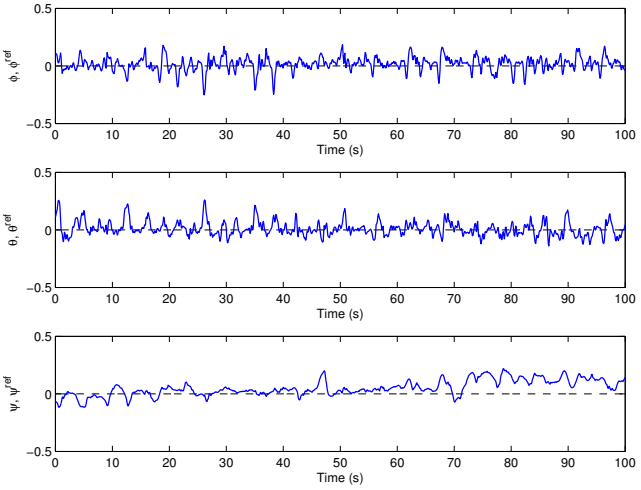

Fig. 6. Attitude regulation subject to a x($1.48m/s$), y($2.69m/s$) and z($1.56m/s$) directional Wind Gust

dynamics and the under–actuated properties of the system make it particularly sensitive to environmental disturbances.

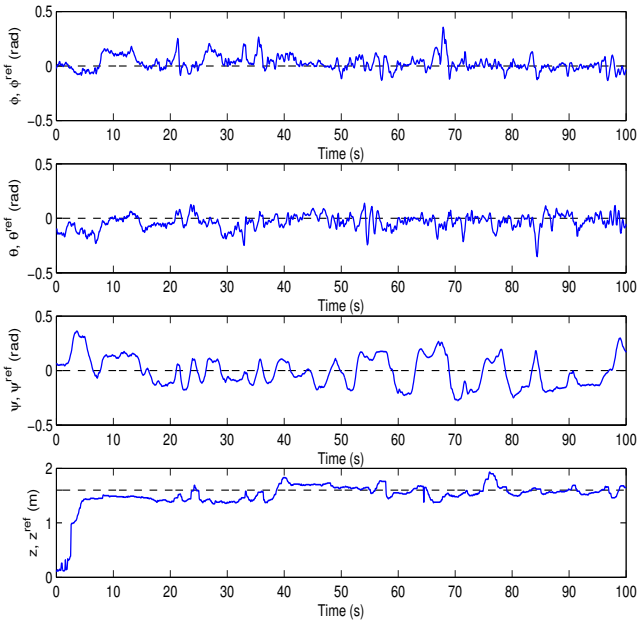

Fig. 7. Stable hover subject to a x($1.48m/s$), y($2.69m/s$) and z($1.56m/s$) directional Wind Gust

Finally, the controller was tested in aggressive attitude regulation. Figure 8 demonstrates the ability of the switching MPC attitude controller to stabilize the quadrotor very fast and accurate even for a great initial roll deviation.

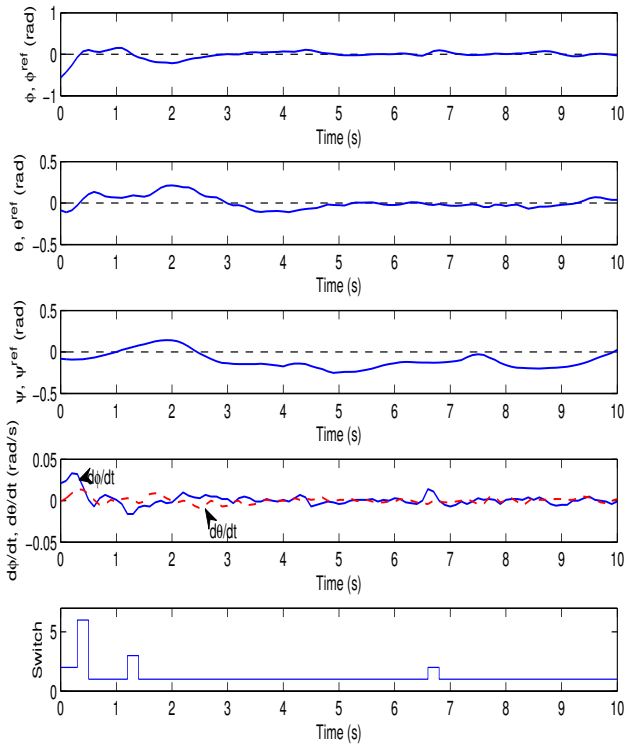

Fig. 8. Aggressive Attitude Regulation Response. The switching among the PWA adopted controllers is shown in the last plot

5. CONCLUSIONS

In this paper, a switching attitude–altitude Model Predictive Controller for a quadrotor has been presented and experimentally verified. The main contribution of the proposed control scheme includes the development of a model predictive controller that counts for the additive environmental disturbances and is computed over a set of linearized Piecewise Affine attitude and altitude models of the system.

ACKNOWLEDGMENTS

This research has been co-financed by the European Union (European Social Fund - ESF) and Greek national funds through the Operational Program "Education and Lifelong Learning" of the National Strategic Reference Framework (NSRF) - Research Funding Program: Heracleitus II. Investing in knowledge society through the European Social Fund. Project number: 12-260-6.

REFERENCES

Alexis, K., Nikolakopoulos, G., and Tzes, A. (2010). Design and experimental verification of a constrained finite time optimal control scheme for the attitude control of a quadrotor helicopter subject to wind gusts. In *2010 International Conference on Robotics and Automation*, 1636–1641. Anchorage, Alaska, USA.

Benallegue, A., Mokhtari, A., and Fridman, L. (2006). Feedback linearization and high order sliding mode observer for a quadrotor UAV. In *International Workshop on Variable Structure Systems (VSS'06)*, 365–372. Alghero, Sardinia.

Bouabdallah, S., Noth, A., and Siegwart, R. (2004). PID vs LQ control techniques applied to an indoor micro quadrotor. In *Proceedings of the IEEE/RSJ International Conference on Intelligent Robots and Systems*, 2451–2456. Sendai, Japan.

Bouabdallah, S. and Siegwart, R. (2007). Full control of a quadrotor. In *2007 IEEE/RSJ International Conference on Intelligent Robots and Systems*, 153–158. doi: 10.1109/IROS.2007.4399042.

Hoffmann, G.M., Huang, H., Waslander, S.L., and Tomlin, C.J. (2007). Quadrotor helicopter flight dynamics and control: Theory and experiment. In *Proc. of the American Institute of Aeronautics and Astronautics (AIAA) Guidance, Navigation, and Control Conference*. SC, USA.

Martin, P. and Salaun, E. (2010). The true role of accelerometer feedback in quadrotor control. In *IEEE International Conference on Robotics and Automation*. Anchorage, Alaska, USA.

P. Bristeau, P. Martin, E.S. and Petit, N. (2009). The Role of Propeller Aerodynamics in the Model of a Quadrotor UAV. In *European Control Conference*. Budapest, Hungary.

Raffo, G., Ortega, M., and Rubio, F. (2010). An integral predictive/nonlinear control structure for a quadrotor helicopter. *Automatica*, 46(1), 29 – 39. doi:DOI: 10.1016/j.automatica.2009.10.018.

Simon, D. (2006). *Optimal State Estimation: Kalman, H infinity and Nonlinear Approaches*. John Wiley and Sons, Hoboken, New Jersey.

Yang, X., Pota, H., and Garrat, M. (2009). Design of a gust–attenuation controller for landing operations of unmanned autonomous helicopters. In *18th IEEE International Conference on Control Applications*, 1300–1305. Saint Petersburg, Russia.